

A Method for Enhancing PET Scan Images Using Nonlocal Mean Filter

Raghad Hazim Hamid¹, Nagham Tharwat Saeed¹, and Hasan Maher Ahmed^{2,*}

¹ Department of Computer Science, College of Education for Pure Science, University of Mosul, Mosul, Iraq; Email: raghad1986@uomosul.edu.iq (R.H.H.); nagham.th@uomosul.edu.iq (N.T.S.)

² Software department, College of Computer Science and Mathematics, University of Mosul, Mosul, Iraq

*Correspondence: hasanmaher@uomosul.edu.iq (H.M.A.)

Abstract—Medical images are an important source of information for both diagnosing and treating diseases. In many cases, the images produced by a Positron Emission Tomography (PET) scan are used to assess the effectiveness of a particular treatment. This paper presents a method for whole-body PET image denoising using a spatially-guided non-local means filter. The proposed method starts with clustering the images into regions. To estimate the noise, a Bayesian with automatic settings of the parameters was used. Then, only patches that belong to regions were collected and processed. The performance was compared to two methods; Gaussian and conventional Non-Local Means (NLM). The Jaszczak phantom and PET/ Computed Tomography (CT) for whole-body were involved in the benchmarking. The obtained results showed that in the Jaszczak phantom, the Signal-to-Noise Ratio (SNR) was significantly improved. Additionally, the proposed method improved the contrast and SNR compared to conventional NLM and Gaussian. Finally, the proposed method, in clinical whole-body PET, can be considered as another way of the post-reconstruction filter.

Keywords—image denoising, image enhancing, medical images, Non-Local Means (NLM) filter, Positron Emission Tomography (PET)/ Computed Tomography (CT) images

I. INTRODUCTION

In recent years, the use of Positron Emission Tomography (PET) scans has become more common, and the images they produce are becoming increasingly important for physicians to understand [1]. This is because these images can show how metabolism and blood flow function in different parts of the body, and they can be used to help diagnose a variety of diseases.

In particular, PET scans are a type of medical imaging that uses radioactive tracers to create images of the body. PET scans are used to track the progress of cancer treatments and to help identify early signs of cancer [2].

The main advantage of PET scans over other imaging methods, such as Computed Tomography (CT) scans, is that they provide a 3D image of the inside of the body, as in Fig. 1 [3]. This enables physicians to more accurately diagnose diseases and plan more effective treatments.

PET scan images can also help to educate people about the importance of this type of imaging, and they can be used to raise awareness about cancer and other diseases. As this technology continues to improve, PET scans will likely play an even more important role in diagnosing and treating diseases [4].

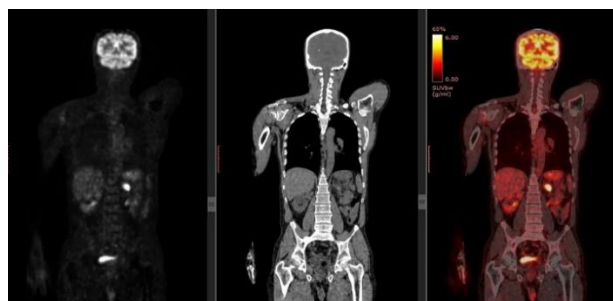


Figure 1. A PET Scan image and a CT scan image.

The processing of PET scan images is a complex task that requires sophisticated software algorithms. Moreover, Computed Tomography (CT) is another type of scan that can provide clear images and detect abnormal cases in soft tissues [5]. As mentioned, PET scans provide images of biological processes. Therefore, PET-CT scans can provide more information about diseases [6].

During the scan procedures, noise is produced in the produced images. This noise causes some difficulties in understanding the images. Therefore, PET-CT scans should be treated and improved to make it clear to physicians [7].

Many techniques are available to reduce the noise in these images such as spatial filtering techniques. They can be used to remove the noise and make images smoother such as through image reconstruction, image thresholding, and image smoothing.

Nonlocal Mean Filtering (NLMF) is an image-processing technique used to reduce noise in digital images. The NLMF filter operates by combining the information from a group of nearby pixels into a single pixel, resulting in a smoother, less noisy image. This process is similar to the averaging of points in statistics, hence the name “nonlocal”. The NLMF filter can be applied selectively to

certain areas of an image, or globally to the entire image. It is a relatively simple and efficient filter.

Moreover, other techniques in the literature can be used for reducing denoise in images such as Chameleon Swarm Algorithm (CSA) [8]. It is driven by the tracking strategies of chameleon's forging. It is considered a "bottom-up clustering approach" that is used for clustering purposes. Moreover, in the literature, it is shown the ability for optimizing problems.

Denosing techniques such as Marine Predators Algorithm (MPA) [9–12] can also be involved. These techniques are "nature-driven optimization approaches".

While other techniques such as Equilibrium Optimizer Algorithm (EOA) [13, 14] can be used for denoising purposes. This kind of technique is a "physics-inspired approach" that is based on physical laws. On the other hand, Grasshopper Optimization Algorithm (GOA) [15] is considered "nature-driven" and used for optimization purposes in the literature.

However, most of the techniques in the literature have limitations in terms of accuracy and complexity. Therefore, it is needed to adopt approaches that provide better accuracy and low complexity aiming to have reliable solutions for problems.

As mentioned, based on the presented works of literature, most of the works need complex calculations or need the parameters to be tuned. Therefore, is needed to have a method that automatically set the parameters and reduces the computational cost. This work suggests a spatial-based that uses a non-local means filter to denoise PET/CT images. The rest of this paper has consisted of the following: Section II presents the proposed research method in detail. Section III describes the experimental results.

II. RELATED WORK

Many research articles have been presented to diagnose diseases in medical images as an important source of information for diagnosis and treatment. In many cases, the images resulting from the imaging examination are used using medical imaging devices, which require improvements to these images. The literature on image denoising includes a lot of works that try to reduce the noise that appeared in PE images.

Cui *et al.* [16] used an unsupervised deep learning technique that does not need to train pairs. Their denoising method used prior information obtained from the same patient. The authors used Gaussian and NLM filters and Contrast-to-Noise Ratio (CNR) and standard deviation metrics to evaluate the performance of their proposed method. The findings showed that unsupervised deep learning methods outperformed Gaussian and NLM methods in image restoration.

In the same context, Kaviani *et al.* [17] proposed a method for the quality enhancement of PET images. Their proposed method was based on the concepts of unsupervised deep learning. They benchmarked the method with other methods in the literature such as Gaussian and NLM using the PNSR metric. The results showed the efficiency of their method. Moreover, images with high noise levels may be obtained from short frame durations [17].

This issue was addressed by Chen *et al.* [18], who proposed an approach that was based on PET data for noise reduction. They compared their approach to other methods such as NLM-ST, STEM, and KIBM5D, and showed their superior performance compared to the benchmarking methods. Watanabe *et al.* suggested a method that used non-local means for comparing the qualitative and quantitative performance of experts. The results showed that for fxPET, the image quality and phantom data were noticeably inferior [19].

In 2020, Arabi and Zaidi presented a paper that suggested using a non-local spatially oriented medium (SG-NLM) technique to solve this issue. The quantitative accuracy and the lesion of the proposed technique were revealed on the Positron Emission Tomography (PET) images of all body parts with different noise levels [20].

In 2022, Hosch *et al.* presented a paper in which full description PET images are generated using ANN and ExtremePET (FDG) images obtained in PET tomography at the time of obtaining results equivalent to that of a computerized scan. A total of 587 patients were treated and a normal and low FDG PET/CT scan was obtained for each patient [21].

In 2022, Mehranian *et al.* presented a paper that enhanced the picture quality of tumor 18F-FDG positron emission tomography scans by applying faster algorithms and deep neural networks to obtain the scans in less time. Data were separated from six centers using GE Discovery PET/CT scanners and the fastest OSEM technology was used to reconstruct short-term data sets [21, 22].

In 2022, Vangu and Momodu presented a paper describing a physiological 18F-FDG polymorphism that may resemble pathology and possibly benign conditions that may cause PET to be misinterpreted for common abdominal and pelvic malignancies. The Warburg effect, which increases anaerobic glycolysis in cancer cells, is exploited by positron emission tomography/computed tomography, which has significantly grown in clinical significance in the majority of cases. These could ultimately have an impact on the accuracy of diagnostic tests for the disease. Various degrees of 18F-FDG are found in the stomach, liver, spleen, and small and large intestines as a result of a normal physiological process [23].

III. METHODOLOGY

The medical imaging technique known as Positron Emission Tomography (PET) reveals the chemical function of an organ or tissue. PET scans can identify malignancies as well as organ dysfunction (such as Alzheimer's disease-affected brain regions or portions of the heart that have been harmed by blood vessel blockage). Fig. 2 shows the main stages of the optimization process.

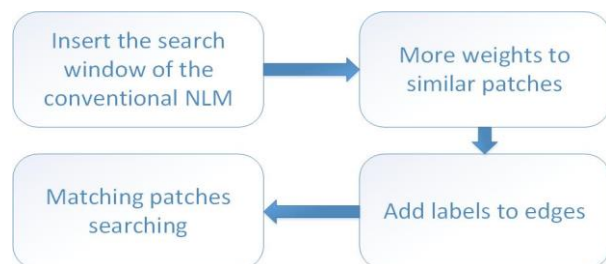


Figure 2. The main steps of the improvement process.

A. Method Steps

Our proposed method includes three main stages and each has its steps. The proposed method starts with estimating noise variance. Using the intensity of the noisy image, the upper bound was estimated.

Based on the technique used in [24–26], this process was performed without the use of any prior knowledge of the level of noise. Also, based on the noisy image's piecewise-smooth version, the noise variance was estimated. Here, we involved the Bayesian MAP framework for creating the correlation between the signal intensity and noise level.

Then, the K-means was used to cluster the piecewise homogenous regions of the noisy image voxels based on spatial connectivity and the similarity of intensity [27, 28]. It should be referred that the clusters were formed based on the variance and mean intensity. After that, all the sample points were involved in the process of estimating the variance of the noise through the fitting function.

The next step of our proposed method is to use the non-local mean filter. The redundant patterns were utilized by the Non-Local Mean (NLM) filter to suppress the noise. Under the use of NLM, the selected patches are averaged aiming to remove the component of the noise component.

This process is performed using the similarity between the nonlocal patches and the patches in the target voxel. The NLM filter works on a spatial constraint called a “Search Window” which can be defined as an image's “fixed sub-dimension” that is used to reduce the search space, which leads to reducing the computations [29, 30].

In the Spatially-Guided NLM (SG-NLM) filter, the concept of a search window does not exist and the searching process is done based on the regions that include the same uptake. Fig. 3 shows the conventional NLM, as can be seen, the wanted voxel is bordered with a green line (search window).

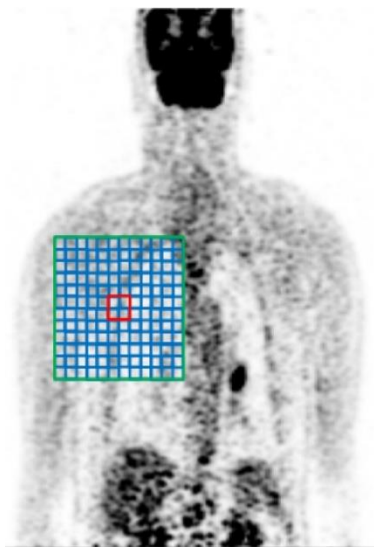


Figure 3. The search window of the conventional NLM.

Moreover, the regions obtained from the previous step were labeled based on the level of intensity from 1 to N. The process of extracting similar patches was performed only on the regions of “same-label”. Fig. 4 shows that the patches are tested and, then, similar patches are assigned more weights.

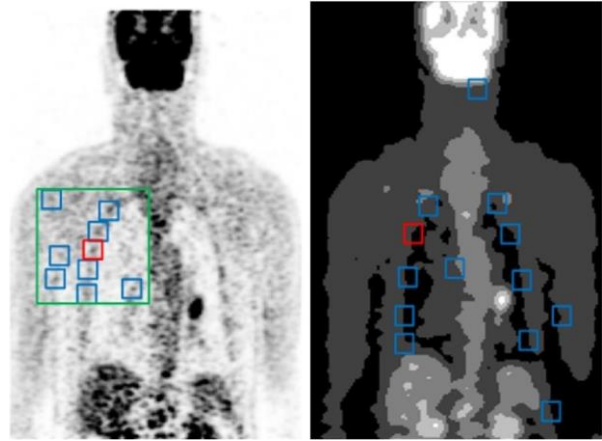


Figure 4. Assigning more weights to similar patches. The target patch is in red.

However, searching for similar patches can be performed only on regions that have similar labels. This process is not restricted only to local regions; it also includes the whole image as shown in Fig. 5.

The Sober edges detector was also used in our work for labeling prominent edges [31, 32] as seen in Fig. 4. The labeling, in this case, depends on whether the target is on the label of an edge. Here, the edges labels were only considered when searching for similar patches, which provided an efficient search in terms of computations consumption as demonstrated in Fig. 6.

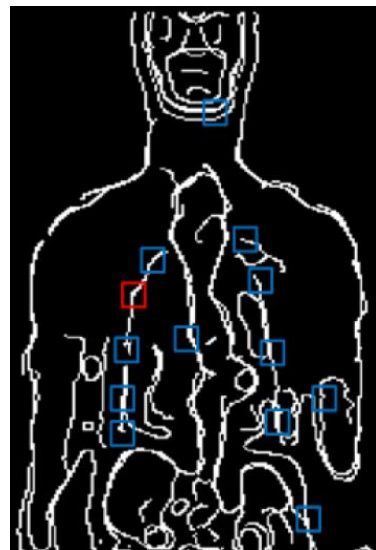


Figure 5. Adding more labels to edges.

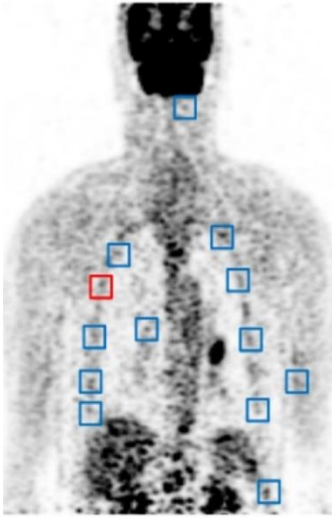


Figure 6. Similar patches searching.

B. Performance Evaluation

The strategy followed in benchmarking the proposed method was based on comparing the SG-NLM with the conventional NLM and Gaussian filters. The metrics used in the evaluation were SNR [33] and CNR [34]. The duration of (15 min, 10 min, and 1 min) was considered for reconstructing the data aiming to vary the noise levels. The physical Jaszczak between the background and spheres was scanned using PET/CT. After applying the method, the difference between the original noise image and the filtered one was calculated for each used filter [35].

Science and engineering employ the signal-to-noise ratio (SNR or S/N) to compare the strength of a desired signal to the strength of background noise as in Eq. (1) and Eq. (2). SNR is referred to as the signal-to-noise ratio and is frequently stated in dB. More signal than noise is indicated by a ratio greater than 1:1 (more than 0 dB).

$$SNR_{dB} = 10 \log_{10} \left[\left(\frac{A_{signal}}{A_{noise}} \right)^2 \right] = 20 \log_{10} \left(\frac{A_{signal}}{A_{noise}} \right) \quad (1)$$

$$SNR_{dB} = 2(A_{signal,dB} - A_{noise,dB}) \quad (2)$$

The Contrast-to-Noise Ratio (CNR) is a metric used to assess the quality of an image, as in Eq. (3). CNR is comparable to the metric Signal-to-Noise Ratio (SNR). This is crucial when there is a clear bias in the image, such as one caused by haze. despite the haze obscuring the image's details, the intensity is fairly high. Consequently, despite having a low CNR metric, this image may have a high SNR meter.

$$C = \frac{|S_A - S_B|}{\sigma_o} \quad (3)$$

where S_A and S_B are signal intensities for signal-producing structures A and B in the region of interest and σ_o is the standard deviation of the pure image noise.

IV. EXPERIMENTAL RESULTS

The experimental results of the Jaszczak phantom filtered are shown in Table I. It can be seen that signal recovery and significant resolution are observed in the SG-NLM approach. The lower performance of the small spheres in terms of loss of contrast was observed in Gaussian.

TABLE I. PERFORMANCE OF THE METHODS (PROPOSED, NLM, AND GAUSSIAN) UNDER DIFFERENT TIMES OF ACQUISITION AS WELL AS THE RESIDUAL IMAGES

Time	Proposed	NLM	Gaussian
15 min			
10 min			
1 min			

TABLE II. SNR AND CNR PERFORMANCE OF THE METHODS USED IN THIS WORK UNDER THE 3 SPHERES

Images	Method	Metric/ Sphere	1	2	3
1	Proposed	SNR	29.1	31.01	33.2
		CNR	14.4	19.7	22.1
	NLM	SNR	27.8	28.9	30.6
		CNR	14.3	18.1	19.9
	Gaussian	SNR	26.2	27.5	28
		CNR	9.4	12.1	14.2
2	Proposed	SNR	28.1	30.01	32.2
		CNR	13.4	18.7	21.1
	NLM	SNR	26.8	27.9	29.6
		CNR	13.3	17.1	18.9
	Gaussian	SNR	25.2	26.5	27
		CNR	8.4	11.1	13.2
3	Proposed	SNR	31.1	32.01	34.2
		CNR	16.4	21.7	24.1
	NLM	SNR	28.8	29.9	32.6
		CNR	15.3	19.1	20.9
	Gaussian	SNR	27.2	28.5	29
		CNR	10.4	14.1	16.2
4	Proposed	SNR	27.2	29.21	31.5
		CNR	12.6	17.7	20.6
	NLM	SNR	25.1	26.4	28.1
		CNR	16.4	16.16	17.2
	Gaussian	SNR	24.8	25.57	26
		CNR	7.8	10.16	12.7
5	Proposed	SNR	31.7	33.61	35.7
		CNR	16.8	19.75	24.6
	NLM	SNR	29.3	30.11	32.2
		CNR	16.6	20.17	21.2
	Gaussian	SNR	28.7	29.58	30
		CNR	11.9	14.23	16.9

As a result, the methods SG-NLM and NLM shows efficient performance with low Table II summarizes the obtained results in terms of the metrics and methods used. The largest sphere shows a higher CNR of (22.1) under the SGNLM.

The smallest sphere reflected a minimum CNR of 9.4 using Gaussian. However, the SG-NLM method demonstrated fewer changes than the other methods in terms of quantification (%) for malignant lesions (Table III).

TABLE III. CHANGE IN THE METHOD USED

Images	Proposed	NLM	Gaussian
1	-2.3	-2.9	-12.3
2	-2.5	-3.0	-13.3
3	-2.1	-2.5	-11.7
4	-2.9	-3.5	-13.5
5	-1.9	-2.1	-10.2

The different results for multiple images and the comparison of SG-NLM with Proposed filters for images were obtained by rating scales SNR and CNR as in Fig. 7, and compared with NLM as in Fig. 8, as well as the comparison with Gaussian as in Fig. 9 by calculating the difference between an image The original noise and image filtered for each filter used.

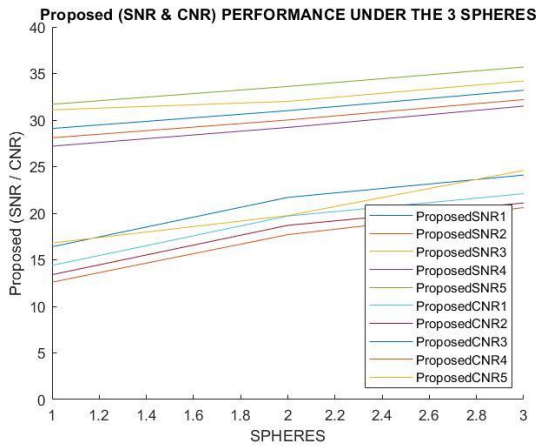


Figure 7. The result of the Proposed (SNR and CNR) for the five images.

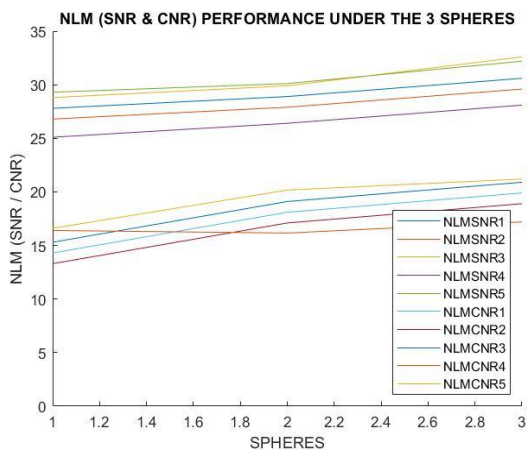


Figure 8. The result of NLM (SNR and CNR) for the five images.

One of the advantages of the proposed method is that it has a step (patch search) that enhances the convolutional NLM. However, the limitation of the proposed approach is that it may consume more time with some types of images or datasets.

Also, the proposed approach can be considered acceptable in terms of complexity compared to the literature. The proposed approach can be developed to be more efficient and reliable even with different types and sizes of datasets.

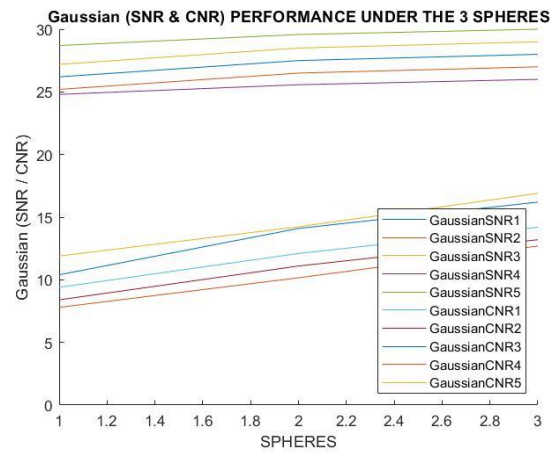


Figure 9. The result of Gaussian (SNR and CNR) for the five images

V. CONCLUSIONS

In this paper, we proposed and tested a non-local mean denoising filter that can efficiently enhance PET/CT images. The proposed method contains many steps, and one of them is patch search, which was able to enhance the efficiency of the conventional NLM. This paper offers a new and improved solution for enhancing PET scan images, which addresses the limitations of existing denoising methods by considering the nonlocal similarity between pixels. The obtained results showed that our method reflected a superior performance compared to conventional NLM and Gaussian denoising.

CONFLICT OF INTEREST

The authors declare no conflict of interest.

AUTHOR CONTRIBUTIONS

Raghad Hazim Hamid, Naghah Tharwat Saeed, and Hasan Maher Ahmed have contributed equally to the conception, design, and execution of the research project. Specifically, Raghad Hazim Hamid contributed to the literature review and data collection, as well as the implementation and testing of the nonlocal mean filter algorithm. Naghah Tharwat Saeed provided technical support and expertise in the field of medical imaging, including the interpretation and analysis of the PET scan images. Hasan Maher Ahmed contributed to the statistical analysis of the results and the writing of the manuscript. All authors have read and approved the final version of the

manuscript and have agreed to be accountable for all aspects of the work.

FUNDING

This work was supported by the University of Mosul.

REFERENCES

- [1] R. Boellaard, R. Delgado-Bolton, and W. J. G. Oyen, "FDG PET/CT: EANM procedure guidelines for tumour imaging: Version 2.0," *European Journal of Nuclear Medicine and Molecular Imaging*, Springer, vol. 42, no. 2, pp. 328–354, 2015, doi: 10.1007/s00259-014-2961-x
- [2] K. J. Friston, C. D. Frith, P. F. Liddle *et al.*, "The relationship between global and local changes in pet scans," *Journal of Cerebral Blood Flow and Metabolism*, vol. 10, no. 4, pp. 458–466, 1990.
- [3] S. Afshari, A. BenTaieb, and G. Hamarneh, "Automatic localization of normal active organs in 3D PET scans," *Comput. Med. Imaging Graph.*, vol. 70, pp. 111–118, 2018. doi: 10.1016/j.compmedimag.09.008
- [4] Z. T. Al-Sharif, T. A. Al-Sharif, N. T. Al-Sharif *et al.*, "A critical review on medical imaging techniques (CT and PET scans) in the medical field," *IOP Conference Series: Materials Science and Engineering*, vol. 870, no. 1, 2020. doi: 10.1088/1757-899X/870/1/012043
- [5] C. I. Lee, A. H. Haims, E. P. Monico *et al.*, "Diagnostic CT scans: Assessment of patient, physician, and radiologist awareness of radiation dose and possible risks," *Radiology*, vol. 231, no. 2, pp. 393–398, 2004. doi: 10.1148/radiol.2312030767
- [6] D. W. Townsend, J. P. J. Carney, J. T. Yap *et al.*, "PET/CT today and tomorrow," *PharmaDeals Rev.*, vol. 45, pp. 4–14, 2004. doi: 10.3833/pdr.v2100i9999.7
- [7] Q. K.-T. Ng, E. K. A. Triumbari, N. Omidvari *et al.*, "Total-body PET/CT—first clinical experiences and future perspectives," *Seminars in Nuclear Medicine*, vol. 52, no. 3, pp. 330–339, 2022.
- [8] B. S. Rao and K. Srinivas, "Medical image enhancement using PCA-based NSCT fusion methodology," *European Journal of Molecular & Clinical Medicine*, vol. 7, no. 11, 2020.
- [9] P.-H. Dinh and N. L. Giang, "A new medical image enhancement algorithm using adaptive parameters," *International Journal of Imaging Systems and Technology*, vol. 32, no. 6, pp. 2198–2218, 2022.
- [10] P.-H. Dinh, "A novel approach using structure tensor for medical image fusion," *Multidimensional Systems and Signal Processing*, vol. 33, no. 3, pp. 1001–1021, 2022.
- [11] P.-H. Dinh, "A novel approach based on three-scale image decomposition and marine predators algorithm for multi-modal medical image fusion," *Biomedical Signal Processing and Control*, vol. 67, 2021.
- [12] P.-H. Dinh, "An improved medical image synthesis approach based on marine predators algorithm and maximum gabor energy," *Neural Computing and Applications*, vol. 34, no. 6, pp. 4367–4385, 2022.
- [13] P.-H. Dinh, "Multi-modal medical image fusion based on equilibrium optimizer algorithm and local energy functions," *Applied Intelligence*, vol. 51, no. 11, pp. 8416–8431, 2021.
- [14] P.-H. Dinh, "Combining gabor energy with equilibrium optimizer algorithm for multi-modality medical image fusion," *Biomedical Signal Processing and Control*, vol. 68, 2021.
- [15] P.-H. Dinh, "A novel approach based on grasshopper optimization algorithm for medical image fusion," *Expert Systems with Applications*, vol. 171, 2021.
- [16] J. Cui, K. Gong, N. Guo *et al.*, "PET image denoising using unsupervised deep learning," *Eur. J. Nucl. Med. Mol. Imaging*, vol. 46, no. 13, pp. 2780–2789, 2019.
- [17] S. Kaviani, M. Mokri, C. Cohalan *et al.*, "Quality enhancement of dynamic brain PET images via unsupervised learning," in *Proc. 13th Biomed. Eng. Int. Conf.*, vol. 10.1109/BM, Ayutthaya, Thailand, 2021, pp. 1–4.
- [18] Z. Chen, Y. Wu, N. Zhang *et al.*, "High temporal resolution total-body dynamic PET imaging based on pixel-level time-activity curve correction," *IEEE Trans. Biomed. Eng.*, pp. 3689–3702, 2022. doi: 10.1109/TBME.2022.3176097
- [19] M. Watanabe, K. Kawai-Miyake, Y. Fushimi *et al.*, "Application of a flexible PET scanner combined with 3 T MRI using non-local means reconstruction: Qualitative and quantitative comparison with whole-body PET/CT," *Mol Imaging Biol.*, vol. 24, no. 1, pp. 167–176, 2022.
- [20] H. Arabi and H. Zaidi, "Spatially guided nonlocal mean approach for denoising of PET images," *Med. Phys.*, vol. 47, no. 4, pp. 1656–1669, 2020. doi: 10.1002/mp.14024
- [21] R. Hosch, M. Weber, M. Sraieb, *et al.*, "Artificial intelligence guided enhancement of digital PET: Scans as fast as CT?" *European Journal of Nuclear Medicine and Molecular Imaging*, vol. 49, pp. 4503–4515, 2022.
- [22] A. Mehranian, S. D. Wollenweber, M. D. Walker *et al.*, "Image enhancement of whole-body oncology [18F]-FDG PET scans using deep neural networks to reduce noise," *Eur. J. Nucl. Med. Mol. Imaging*, vol. 49, no. 2, pp. 539–549, 2022. doi: 10.1007/s00259-021-05478-x
- [23] M. Vangu and J. Momodu, "F-18 FDG PET/CT Imaging in Normal Variants, Pitfalls and Artifacts in the Abdomen and Pelvis," *Front. Nucl. Med.*, vol. 1, pp. 1–12, 2022, doi: 10.3389/fnume.2021.826109
- [24] R. Boellaard, R. Delgado-Bolton, W. Oyen *et al.*, "FDG PET/CT: EANM procedure guidelines for tumour imaging: version 2.0," *Eur J Nucl Med Mol Imaging*, vol. 42, no. 2, pp. 328–354, 2015. doi:10.1007/s00259-014-2961-x
- [25] J. Krislynd, S. Aprianto, and D. Suhartono, "A comparative study of various convolutional neural network architectures for eye tracking system," *Journal of Image and Graphics*, vol. 10, no. 4, pp. 178–183, 2022. doi: 10.18178/joig.10.4.178-183
- [26] C. Liu, W. Freeman, R. Szeliski *et al.*, "Noise estimation from a single image," in *Proc. IEEE Comput. Soc. Conf. Comput. Vis. Pattern Recognit.*, vol. 1, 2006, pp. 901–908. doi: 10.1109/CVPR.2006.207
- [27] Y. Izumi, D. Suto, S. Kawakami *et al.*, "Blind image restoration and super-resolution for multispectral images using sparse optimization," *Journal of Image and Graphics*, vol. 10, no. 1, 10–16, 2022. doi:10.18178/joig.10.1.10-16
- [28] C. Zitnick, N. Jovic, and S. Kang, "Consistent segmentation for optical flow estimation," in *Proc. IEEE Int. Conf. Comput. Vis.*, vol. II, no. November, 2005, pp. 1308–1315. doi: 10.1109/ICCV.2005.61
- [29] J. She and Y. Liu, "Facial image inpainting algorithm based on attention mechanism and dual discriminators," *Journal of Image and Graphics*, vol. 10, no. 1, pp. 43–49, 2022. doi: 10.18178/joig.10.1.43-49
- [30] Z. Xu, M. Gao, G. Papadakis *et al.*, "Joint solution for PET image segmentation, denoising, and partial volume correction," *Medical Image Analysis*, vol. 46, pp. 229–243, 2018. doi: 10.1016/j.media.2018.03.007
- [31] J. Wu, G. Li, T. Kamiya, "Multi-organ statistical shape model building using a non-rigid ICP based surface registration," *Journal of Image and Graphics*, vol. 10, no. 3, pp. 95–101, 2022. doi: 10.18178/joig.10.3.95-101
- [32] H. Spontón and J. Cardelino, "A review of classic edge detectors," *Image Process. Line*, vol. 5, pp. 90–123, 2015. doi: 10.5201/ipol.2015.35
- [33] N. Ibrahim, A. Darlis, and B. Kusumoputro, "Performance analysis of fuzzy-weighted multiple instance learning on thermal video-based visual tracking," *Journal of Image and Graphics*, vol. 10, no. 2, pp. 88–94, 2022. doi: 10.18178/joig.10.2.88-94
- [34] P. Kellman and E. McVeigh, "Image reconstruction in SNR units: A general method for SNR measurement," *Magn. Reson. Med.*, vol. 54, no. 6, pp. 1439–1447, 2005. doi: 10.1002/mrm.20713
- [35] A. Geissler, A. Gartus, T. Foki *et al.*, "Contrast-to-Noise Ratio (CNR) as a quality parameter in fMRI," *J. Magn. Reson. Imaging*, vol. 25, no. 6, pp. 1263–1270, 2007. doi: 10.1002/jmri.20935

Copyright © 2023 by the authors. This is an open access article distributed under the Creative Commons Attribution License ([CC BY-NC-ND 4.0](https://creativecommons.org/licenses/by-nc-nd/4.0/)), which permits use, distribution and reproduction in any medium, provided that the article is properly cited, the use is non-commercial and no modifications or adaptations are made.